1972PASAu...2...84D

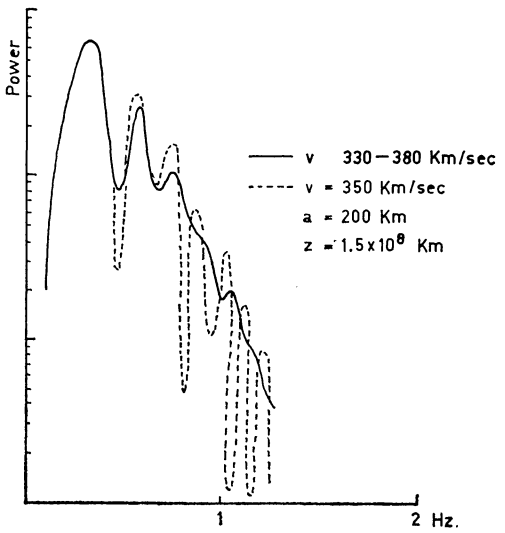

Figure 3. The effect of a random velocity field in a thin scattering layer for an observing frequency of 80 MHz. The minima in the constant velocity spectrum do not extend to zero because of the finite resolution (0.05 Hz) imposed during computation.

to the difficulties. An examination of our own data indicates that under normal conditions of the interplanetary medium, neither a Fourier nor a Bessel analysis of observations at 80 MHz is able to yield any significant modulation pattern. It appears that only under unusual circumstances might the technique be at all useful at this frequency. Such a situation arose however in May 1968, when a corotating plasma stream approached the Earth[2] and low frequency dips were seen in the scintillation power spectra of the source 0134 + 32. These were interpreted as evidence for the proximity of the scattering region, i.e. that the Earth was located within the Fresnel region, and allowed the screen to be placed at $Z \sim 0.1$ A.U. These data have been analysed further by computing the Bessel transform, not of the autocorrelation function, but from the one-dimensional Fourier power spectrum using a sec θ transform,

$$P(f) = -\frac{\mathrm{d}}{\mathrm{d}f}\int_0^{\pi/2} P_F(f \sec\theta)\,\mathrm{d}\theta\,.$$

These two procedures have been shown to be exactly equivalent,[10] the sec θ transform being preferred because of its computational simplicity. The computed spectrum from these observations is shown in Figure 4. Above 1.4 Hz the spectrum becomes statistically unstable, but below this limit four minima are seen which closely fit the $\sqrt{n}$ dependence of equation (2), and which correspond to $n = 0$, 1, 2 and 3. Taking $Z = 0.1$ A.U., a velocity of 315 km/s is derived. It would appear that this was a rather rare occurrence in which the effective screen was thin due to the presence of the corotating stream and, as mentioned above, sufficiently close to the Earth that observations were within the Fresnel region.

At 80 MHz for the scattering to be weak, observations must be made at elongations $\gtrsim 30°$ so that generally the geometrical smearing effect will be important. At higher frequencies conditions are more favourable for the observation of modulation in the power spectrum. At frequencies ~ 1 GHz, observations to within 10° or less of the Sun could be made: the geometrical effect would become negligible and the smaller scale of the irregularities would allow minima to be observed out to higher spatial frequencies. On the other hand there is some evidence that within 30 $R_\odot$ turbulent velocities become important, and this may become the major cause of blurring as indicated in Figure 3.

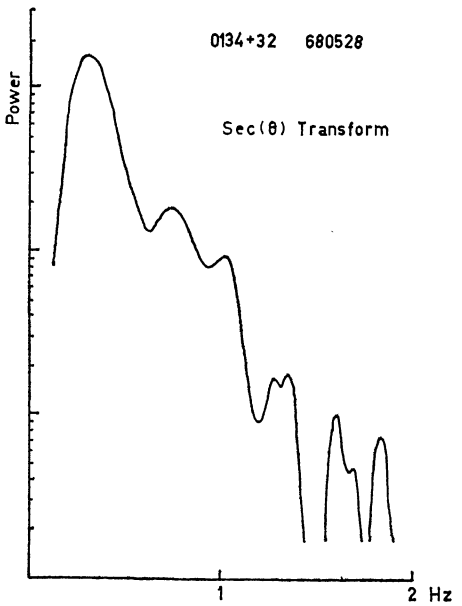

Figure 4. An experimental power spectrum computed using the sec θ transform, from observations at 80 MHz during May, 1968.

We wish to thank Dr R. Buckley for many invaluable discussions on spectral analysis and also the CSIRO, Division of Radiophysics for the provision of observing facilities on the Radioheliograph, Culgoora. One of us (R.G.B.) acknowledges the support of a Commonwealth Postgraduate Award.

[1] Little, L. T. and Hewish, A., *MNRAS*, **138**, 393 (1968).
[2] Dennison, P. A. and Wiseman, M., *Proc. ASA*, **1**, 142 (1968).
[3] Wiseman, M. and Dennison, P. A., *Proc. ASA*, **2**, 79 (1972).
[4] Lovelace, R. V. E., Salpeter, E. E., Sharp, L. E. and Harris, D. E. *Ap. J* **159**, 1047 (1970).
[5] Rufenach, C. L., Ph.D. Thesis, University of Colorado, 1971.
[6] Bowhill, S. A., *J. Res. N.B.S. (Rad. Sci.)*, **D65**, 275 (1961).
[7] Salpeter, E. E., *Ap. J.*, **147**, 433 (1967).
[8] Readhead, A. C. S., *MNRAS*, **155**, 185 (1971).
[9] Golley, M. G. and Dennison, P. A., *Planet. Space Sci.*, **18**, 95 (1970).
[10] Buckley, R., Private Communication.
[11] Ekers, R. D. and Little, L. T., *Astron. Astrophys.*, **10**, 310 (1971).

Coronal Broadening of the Crab Nebula 1969-71

Observations

R. G. Blesing and P. A. Dennison
Department of Physics, University of Adelaide

A description was given in a previous paper[1] of the first observations of the two-dimensional image of the Crab Nebula as it became broadened by the solar corona in June 1969. In this paper we describe further observations at 80 MHz during 1970 and 1971, again using the CSIRO

© Astronomical Society of Australia • Provided by the NASA Astrophysics Data System

1972PASAu...2...84D

Radioheliograph[2] at Culgoora, N.S.W., and we discuss the derived values for radial and tangential broadening in relation to previous work at various phases of the solar cycle. Other methods of observing angular broadening[3] have generally employed two or three interferometers at different position angles, and only the simplest model for the image could be assumed in interpreting the results. The radioheliograph, however, has the advantage of recording the complete two-dimensional image and also, simultaneously, the surrounding background.

Data were recorded both photographically, from a cathode ray tube display, and digitally on magnetic tape for subsequent analysis by computer. While recording the original data the field of view was scanned at the rate of $2s^{-1}$ or $1s^{-1}$, but for the photograph records the data were integrated over eight frames to improve the signal-to-noise ratio. Much better signal-to-noise ratios could have been obtained by integrating a larger number of frames but over such longer periods ionospheric refraction would, on some occasions, have broadened the image by several mins arc, giving misleading results.

Typical pictures of the broadened source have been combined in Figure 1* by placing them in their correct positions relative to the Sun, to produce a composite picture summarizing the near-occultations of the Crab Nebula for each of the three years. The different alignments of the background grid, which can be seen on different pictures, result from corrections having been applied to compensate for the distortion of the field of view when observed away from the meridian. By comparing observations at the same radial distance from the Sun for each of the three years, it is clear that the scattering was significantly reduced during 1971, whilst it remained approximately the same during 1969 and 1970. This is a reflection of the decline of the solar cycle during the last year. It is also clear from Figure 1 that during 1969 and 1970 the scattering was so strong that within about 8 $R_\odot$ the source could not be resolved above the background noise level.

As the source approached the Sun the image became elongated indicating the presence of filamentary irregularities in the corona. In general the orientation of the scattering ellipse was in the tangential direction indicating a radially aligned magnetic field. One exception was clearly the 12th, 1970, where the image was aligned almost in the N-S direction. This event will not be described here but is believed to be related to the presence of an active region on the Sun.

Although the photographic records provide a useful summary of the observations they are not suitable for more detailed analysis. Such quantitative work has been based entirely on the magnetic tape records. Sections of data ranging from 5 to 20 min. in duration were analysed by first integrating over 15 or 30 sec., and then fitting the integrated image to an elliptical Gaussian model by the method of least squares. Although this model did not allow for the slight curvature of the image, tests proved that the errors introduced were negligible, particularly at larger radial distances. The parameters determined in this way were the background intensity, the peak intensity of the image, the tangential and radial widths and the orientation. The beam shape and the natural source size were deconvolved leaving the scattering ellipse. Values of the

*See Plate I.

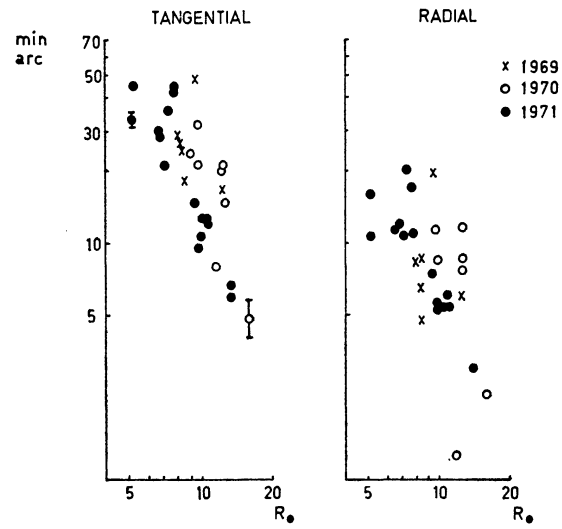

Figure 2. Values of the radial and tangential broadening (full-width, e^{-1}) during 1969-71 at 80 MHz.

tangential and radial broadening (full width at e^{-1}) for the three years are shown in Figure 2, together with typical error bars. The 1971 values are seen to be in general lower than the 1969 and 1970 values.

Lines of best fit were calculated for the tangential scattering values of 1971 and for the combined 1969–70 tangential values. After scaling to a frequency of 38 MHz assuming a λ^2 dependence of the scattering, these lines are shown in Figure 3 together with the results of other authors[3] at different phases of the solar cycle. Good

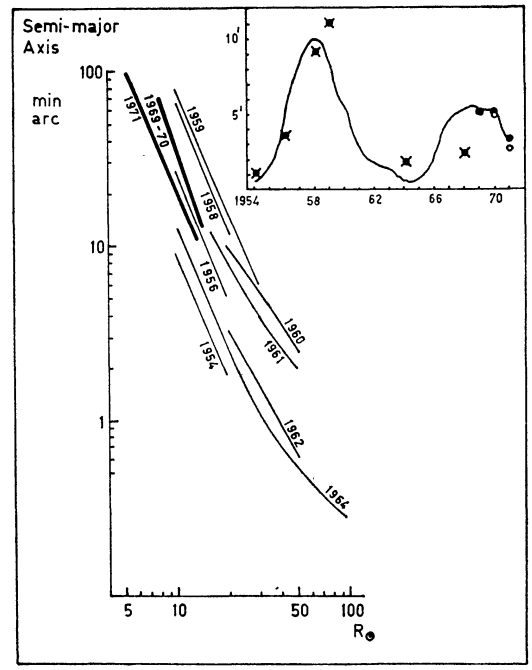

Figure 3. Our values of the tangential broadening (heavy lines), scaled to 38 MHz for comparison with earlier work at various phases of the solar cycle. *Inset* values of the radial broadening at 12 $R_\odot$ and at 80 MHz compared to smoothed sunspot number; • the present observations; o Matheson and Little,[4] x Okoye and Hewish.[3]

© Astronomical Society of Australia • Provided by the NASA Astrophysics Data System

1972PASAu...2...84D

agreement is apparent both for the degree of scattering at the relevant part of the solar cycle and for the slope of the lines. To illustrate further the solar cycle variation, the inset to Figure 3 shows our values for the radial scattering angle at 12 $R_\odot$ compared to those of other authors[3, 4] over the past 18 years. It is seen that the degree of scattering shows good agreement with the smoothed sunspot numbers for these years.

Lines of best fit were also calculated for the radial scattering values giving a mean slope of −1.6 for the three years. This value may be compared to the slopes −2 and −3, calculated for the tangential broadening in 1969–70 and 1971 respectively. The different radial variations of radial and tangential scattering suggest that the axial ratio of the scattering irregularities may increase close to the Sun.

The results above have been obtained by assuming a tangentially aligned image, and in fact the variation of the major axis from the tangential direction was found to be random with a rms deviation of $\sim 5°$.

We have presented a brief outline of three years of observations of the Crab Nebula during its near-occultation by the Sun. The scattering data agree well with results of other authors for previous years and extends the amount of information which can be obtained from angular broadening observations. The interpretation of the results in terms of various scattering models and a discussion of the variation of axial ratio of the plasma irregularities will be given in the following paper.

It is a pleasure to extend our thanks to the CSIRO, Division of Radiophysics for providing observing facilities on the Radioheliograph. One of us (R.G.B.) acknowledges the support of a Commonwealth Postgraduate Award.

[1] Harries, J. R., Blesing, R. G. and Dennison, P. A., *Proc. ASA*, **1**, 319 (1970).
[2] Wild, J. P. *et al.*, *Proc. IREE Aust.*, **28**, No. 9 (1967).
[3] Okoye, S. E. and Hewish, A., *MNRAS*, **137**, 287 (1967).
[4] Matheson, D. N. and Little, L. T., *Nature*, **234**, 29 (1971).

Coronal Broadening of the Crab Nebula 1969-71
Interpretation

P. A. Dennison and R. G. Blesing
Department of Physics, University of Adelaide

In the preceding paper,[1] observations of the coronal broadening of the Crab Nebula during 1969-71 were described. The basic parameters, radial and tangential broadening, and their relation to previous work were discussed. Whereas previous observations have utilized two or three interferometers only, so that the degree of broadening along any particular axis could only be obtained under the assumption of a particular form (e.g. Gaussian) for the angular power spectrum, the present work has enabled complete sampling of the two-dimensional brightness distribution of the broadened source. It is therefore possible, and of considerable interest, to compare the observed distributions to those computed on the basis of various theoretical models for the scattering process.

The simplest case to treat is that of an angular spectrum which has Gaussian cross-sections. The relation between the angular spectrum and the spatial power spectrum of the scattering irregularities is well known,[2] and the Gaussian angular spectrum we consider first is equivalent to a

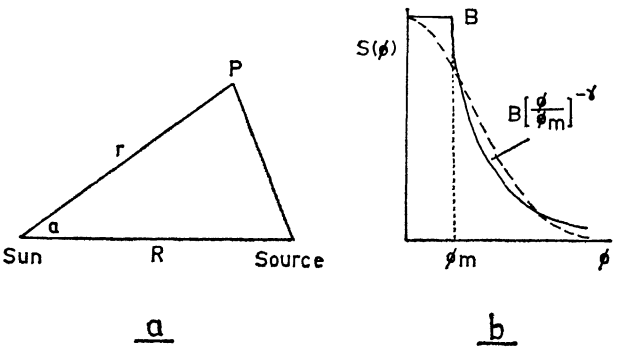

Figure 1. (a) The scattering geometry. (b) Parameters of the power-law model for the angular spectrum with a Gaussian curve shown for comparison.

Gaussian spectrum for the scattering irregularities. This model implies, therefore, a single dominant scale structure for the plasma irregularities.

In Figure 1(a) are shown the Sun and the Crab Nebula as seen projected onto the celestial sphere. It is required to calculate the brightness $B(r,\alpha)$ of all points $P(r,\alpha)$ around the true source position. We assume that the scattering gives rise to an angular spectrum of the form $\exp -(\phi^2/\phi^2_0)$, and that ϕ_0 has an elliptical distribution in the (r,α) plane with semi-axes $\phi_0(r)$ and $\phi_0(t)$ in the radial and tangential directions respectively. ϕ_0 is inversely proportional to the scale of the scattering irregularities so that, for example, radially elongated structures in the interplanetary plasma result in $\phi_0(t) > \phi_0(r)$.

Observationally it was shown in the previous paper that ϕ_0 may be represented by a power law such that

$$\phi_0(r) = \frac{r^{-S}}{A} \text{ and } \phi_0(t) = \frac{r^{-T}}{B}.$$

On this basis we can calculate the brightness of points $P(r,\alpha)$, finding the result

$$B(r,\alpha) = C/\{(A^2r^{-2S} + \theta^2)(B^2r^{-2T} + \theta^2)\}^{1/2} \times \exp -\{r^2 + R^2\cos^2\alpha - 2rR\cos\alpha) \times (A^2r^{-2S} + \theta^2)^{-1} + R^2\sin^2\alpha/(B^2r^{-2T} + \theta^2)\} \quad (1)$$

In deriving equation (1) a convolution has been performed with a source distribution $\exp -(\phi^2/\theta^2)$. For comparison with the observed brightness distributions, $B(r,\alpha)$ has been computed as a function of distance R from the Sun, and the parameter $X = A/B$. For isotropic scattering $X = 1$, and for radially elongated plasma irregularities $X > 1$. Some examples of these theoretical distributions are shown in Figure 2, where parameters have been used typical of the 1969 observations,

$$S \simeq T \simeq 2$$
$$B \simeq 1.8 \times 10^5$$
$$\theta \simeq 5.14 \times 10^{-4}$$

where all angles are expressed in radians.

In comparing such distributions with our observational data we find closest agreement using values of the elongation parameter $X = 2 - 3$. Results of such a comparison were presented at the 1970 IAU General Assembly, and we are now able to discuss the results of a more complete analysis for 1970 and 1971 data.

In Figure 3 are shown three examples of observed brightness distributions in the form of contour diagrams computed from the data recorded on magnetic tape. Beneath

© Astronomical Society of Australia • Provided by the NASA Astrophysics Data System